A computationally efficient treatment of a polarizable metallic electrode held at a constant potential.

Matt K. Petersen[1],* Gregory A. Voth[1], and Henry S. White[2]

[1] *University of Chicago, Department of Chemistry*

[2] *University of Utah, Department of Chemistry*

Abstract

We present a computationally efficient method for the treatment of electrostatic interactions between a polarizable metallic electrode held at a constant potential and an electrolyte. In short, the method combines a fluctuating uniform electrode charge with explicit images charges to account for the polarization of the electrode by the electrolyte, and a constant uniform charge added to the fluctuating uniform electrode charge to account for the constant potential condition. The method is then used to calculate electron transport rates using Marcus theory.

*Electronic address: mkpetersen@chicago.edu

I. INTRODUCTION

Several simplifying approximations have been made when treating the electrode/electrolyte interface within classical molecular dynamics simulations. The most straightforward approach, in concept and implementation, have been to model the electrode as a uniformly charged plane[1]. More advanced treatments have further included a treatment of the atomically corrugated electrode surface[2, 3], or modeled the electrode surface as a collection of atomic sites bearing partial charges contributing to the total electrode charge[4–6] While computationally inexpensive and conceptually simple, these approaches fail to capture the dispersion interactions between the electrolyte and the electrode, with potentially significant impact ion the structure of the electrical double layer at the electrode[7].

One method, the so-called "method of images", does account for the polarization of the electrode by the electrolyte[3, 7, 8]. In this method, a static image plane is defined - typically coincident with the nuclear plane of the electrode surface. For each charge in the system q_i there is a corresponding image charge such that $q_{img} = -q_i$. The interactions of all non-image charges in the system, whether they are partial charges of the constituent atoms of an electrolyte molecule or ionic charges, are included between all image charges as well as all real charges. While the method does correctly account for the polarization of the electrode by the electrolyte, the method can only model a charged electrode when the electrolyte has a net charge[9, 10]. It should be noted that creating a fixed charge on the electrode, either by applying a uniform charge to the electrode or through the image charges of an electrolyte with a net charge, cannot correctly account for the electrode charge due to an imposed *constant potential*. As we will show below, the correct charge distribution can be correctly modeled by a combination of the two methods given specific simulation constraints.

An approach capable of modeling a polarizable charged electrode adjacent to a non-neutral electrolyte has been formulated by Siepmann and Sprik,[11] and applied to bulk simulations of a complete electrochemical cell by Reed et al.[12] In short, this method models the electrode as a series of Gaussian charge distributions centered about the nuclear positions of the electrode atoms. The charge on each electrode atom at each simulation time-step is obtained by enforcing a *constant potential* at the electrode atoms. While this method accurately reproduces the charge distribution within the electrode, it is computationally expensive. Below we describe a method that quantitatively reproduces the results of Reed

et al.[12, 13] without the expense of the iterative minimization of the system potential, or otherwise using polarizable atomic potentials.

II. METHODS

A. The Model

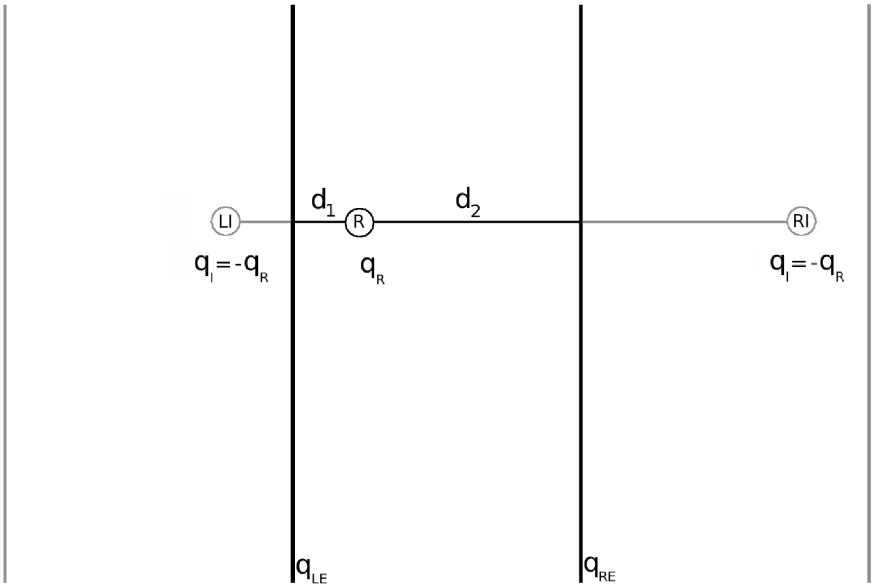

FIG. 1: Electrochemical cell.

Consider an electrochemical cell composed of two *parallel* electrodes and intervening electrolyte (Fig. 1). This cell consists of two electrodes; the left electrode (LE) located at $z = 0$, and the right electrode (RE) located at $z = D$, both periodic in the x and y dimensions. A charged atom of the bulk electrolyte (R), located at the position $(0, 0, z_R)$ with charge q_R, will induce a charge on the surface of the conducting electrodes. This induced surface charge will create a potential equivalent to one where a charge $q_I = -q_R$ is located equidistant from the electrode surface, but within the electrode.[14] That is, the real electrolyte charge R will induce a surface charge in the two electrodes creating a potential equal to that created by a pair of image charges, RI and LI. These image charges will have charge $q_I = -q_R$, located at $(0, 0, -z_R)$ and $(0, 0, d_1 + 2d_2)$, such that $d_1 = z$, d_2 is the distance of the real charge from electrode RE, and $D = d_1 + d_2$ is the distance between

electrode LE and RE.

The above consideration does not account for the possibility of the primary image charges of one electrode inducing secondary image charges in the opposing electrode, which in turn can create further image charges in the first, and so on. As we will show in the following discussion, these higher order image charges will be accounted for as part of the constant potential constraint and through the treatment of the long range electrostatic interactions.

The electric field within the electrochemical cell can be found from the charge distribution from within the cell (Eqtn. 1);

$$E(z) = \frac{1}{\epsilon_0} \int \rho(z) dz. \tag{1}$$

For a cell composed of discrete charges,

$$\rho(z_i^*) = \frac{q_i(z_i^*)}{A \Delta z_i}, \tag{2}$$

where $q(z_i^*)$ is the discrete charge at the point z_i^* on the interval Δz_i. The electric field is then,

$$E(z) = \frac{1}{\epsilon_0 A} \int_0^D \frac{q(z_i^*)}{\Delta z_i} dz = \frac{1}{\epsilon_0 A} \lim_{\Delta z_i \to 0} \sum_{i=1}^{p} \left(\frac{q_i(z_i^*)}{\Delta z_i} \right) \Delta z_i, \tag{3}$$

such that,

$$\sum_{i=1}^{p} \Delta z_i = D \tag{4}$$

for p partitions. When the electric field is integrated over the entire cell, the electric field just inside the second electrode is

$$E(D) = \frac{1}{A\epsilon_0} \left(q_{RE} + q_{LE} + \sum_{i=1}^{n} q_{R_i} + 2 \sum_{i=1}^{n} q_{I_i} \right) = \frac{1}{A\epsilon_0} \left(q_{RE} + q_{LE} - \sum_{i=1}^{n} q_{R_i} \right), \tag{5}$$

where q_{LE} and q_{RE} are the charges induced on the surface of the left and right electrodes by the n charges of the electrolyte, excluding *primary* images charges. And since the electric field inside a conductor is 0,

$$\sum_{i}^{n} q_{R_i} = q_{RE} + q_{LE}. \tag{6}$$

The electrical potential across the electrochemical cell can be found from the electric field,

$$\Phi(z) = - \int E(z) dz. \tag{7}$$

Using the expression for the electric field from Equation 3,

$$\Phi(z) = -\frac{1}{\epsilon_0 A}\int_0^D \lim_{\Delta z_i \to 0} \sum_{i=1}^{p} \left(\frac{q_i(z_i^*)}{\Delta z_i}\right) \Delta z_i = -\frac{1}{\epsilon_0 A} \lim_{\Delta z_j \to 0} \sum_{j=1}^{p} \left(\sum_{i=1}^{j} q_i(z_i^*)\right) \Delta z_j. \tag{8}$$

Integrated over the entire cell, the potential is

$$\Phi(D) = -\frac{1}{\epsilon_0 A} \sum_{i}^{n=1} \Big[\left(-q_{R_i} + q_{LE_i}\right)\left(z_{R_i}\right) + \left(q_{LE_i}\right)\left(D - z_{R_i}\right) \Big], \tag{9}$$

where q_{LE_i} is the surface charge induced by the higher order images resulting from the *ith* charge of the electrolyte on electrode LE such that,

$$q_{LE} = \sum_{i}^{n=1} q_{LE_i}. \tag{10}$$

Using the equality from Equation 6 and accounting for the constant potential drop, ΔV_0, across the cell,

$$\Delta V_0 = \frac{1}{\epsilon_0 A} \Big[\sum_{i}^{n} -q_{R_i} z_{R_i} + (q_{LE})(D) \Big]. \tag{11}$$

If we express the constant potential in terms of the electrode charge, Q_0, of an equivalent *capacitor*,

$$\Delta V_0 = \frac{Q_0}{\epsilon_0 A} D, \tag{12}$$

and use the equality from Equation 6 to write the electrode charges in terms of the electrolyte charges,

$$q_{EL} = \sum_{i=1}^{n} \frac{q_{R_i} z_{R_i}}{D} + Q_0, \quad q_{ER} = \sum_{i=1}^{n} q_{R_i} \left(1 - \frac{z_{R_i}}{D}\right) - Q_0. \tag{13}$$

Equations 13 are the primary result of the analysis. To summarize, assuming two parallel electrodes, an intervening electrolyte of discrete charges, and that primary image charges are induced on each electrode, then the total charge of the higher order images charges are equal to the total of the electrolyte charge. This is a seemingly a trivial conclusion. If it were not so, then the cell would have created charge. More importantly though, Equations 13 show that the total electrolyte charge is shared between the electrodes in proportion to the position of the center of electrolyte charge. This is a very useful result when faced with modeling charge transfer in the cell. When charge is transferred from the electrolyte to the electrode in the course of a simulation, it isn't immediately apparent how it should be done. What Equations 13 show is that the charge is transferred to *both* electrodes, and

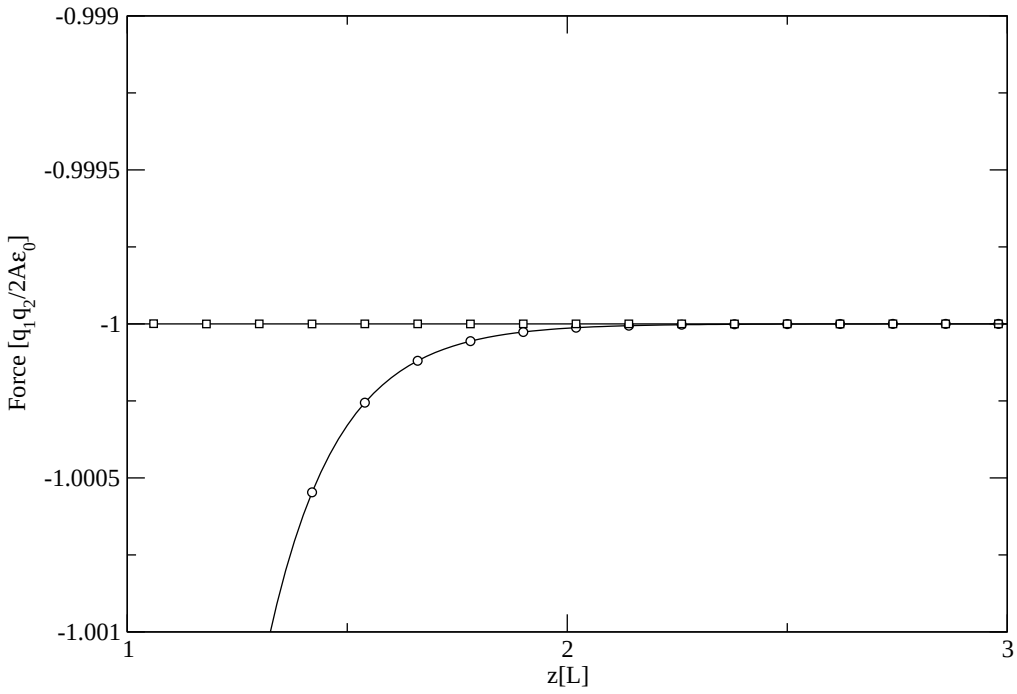

FIG. 2: Force experienced by a point charge from a point charge (circles) of equal charge, and from a charged wall (squares) of equal charge.

the amount of charge transferred to each is proportional to the position of the transferring species within the cell. This position dependence has been demonstrated by Reed et al.[13], albeit as an imperial observation of their model. We have shown that this dependence is an *a prior* consequence of the constant potential boundary condition.

Unfortunately, Equations 13 don't show how this charge is distributed on the surface of the electrode. Considering the charge induced on the surface of the electrodes by the electrolyte was initially assumed to be correctly described by the primary image charges, how then should the charge induced by the opposing electrodes themselves be modeled?

Figure 2 shows the force (circles) experienced by a test charge, $q_1 = e^-$,located at $(0, 0, z)$ due to another charge, $q_2 = -q_1$, located at $(0, 0, 0)$, as a function of the separation, z. Also shown is the force (squares) experienced by the same test charge due to a charged wall composed of a 10 by 10 array of atoms located at $(x, y, 0)$ arranged in a simple cubic lattice with a net charge of $-q_1$. These data were collected for systems which were periodic in the x and y dimension such that L_x=L_y, and non-periodic in the z dimension. The length and force in Figure 2 have been normalized to $\mathrm{L}_{x,y}$ and $\frac{q_1 q_2}{A\epsilon_0 2}$ - the force due to a uniformly charged wall - respectively.

At large enough separation, the array of periodic images of the higher order image charges should appear as a uniformly charge wall. From Figure 2 we see this occurs at a length equivalent to one to two periodic images. Approximating the images as a uniformly charged plane has been used to treat *primary* images at separations where $z > min(L_x, L_y)$[15]. Reed et al. have shown that the higher order image charges are uniformly distributed over the entire electrode even at lengths roughly equal to the x and y periodic lengths[12]. Since, at their closest, the separation between the real and higher order images charges is never greater that the electrode separation, D, approximating the induced surface charge, q_{EL} and q_{ER}, as uniformly distributed is a reasonable approximation.

B. Validation

Initial validation of the model consists of a comparison with the more sophisticated, albeit computational more intensive model of Reed et al[12, 13]. In short, the model of Reed et al. allows for the polarization of the metallic electrode through variable Gaussian charge distributions which are adjusted according to a variational procedure, accounting for the constant potential condition of the electrodes. The key differences between the model of Reed et al. and that proposed here is the way the electrode charges are adjusted and the use of explicit image charges in the proposed model. Where Reed et al. meet the constant potential condition by minimizing the total potential of the system by adjusting the atomic charge of the electrode, the proposed model adjusts the electrode atomic charges according to Equations 13. And while the model of Reed et al. intrinsically arrives at the electrode surface charge distribution commensurate with that of an image charge, the proposed model uses explicit image charges, updated according to the position of the corresponding electrolyte charges, to mimic the nonuniform portion of the electrode surface charge distribution. The details of the image charge scheme, treatment of long range electrostatics, and so forth are discussed in detail in the Computation section.

Two validation systems have been created to investigate the accuracy of the proposed model; System I is composed of two parallel electrodes separated by a distance D=52.9 Å. The electrodes are composed of three layers of atoms (a total of 2700 atoms) arranged in a fcc lattice with a lattice parameter of 3.92 Å. Each electrode is periodic in the x and y dimensions such that x = 83.1 Å and y = 72.0 Å, with the (111) face exposed to the

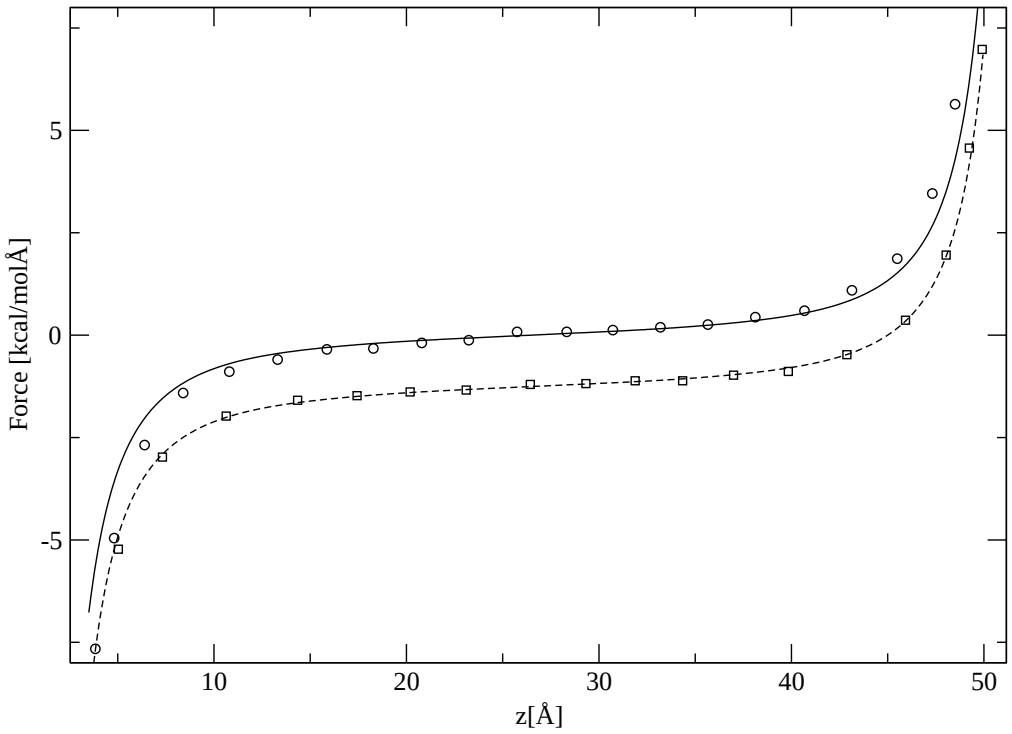

FIG. 3: Force experienced by the test charge in System I as a function of the position in the cell. Propose method (lines), and the method of Reed et al. (symbols). $V_0 = 0.0V$ (solid line and circles), $V_0 = 2.75V$ (dashed line and squares).

electrolyte. A single charge, $q_R = -e$ is located at $(0, 0, z)$ in the space between the two electrodes. System II is composed of two parallel electrodes separated by a distance D=85.0 Å. The electrodes are composed of three layers of atoms (a total of 294 atoms) arranged in a fcc lattice with a lattice parameter of 3.66 Å. Each electrode is periodic in the x and y dimensions such that $x = 25.62$ Å and $y = 25.62$ Å, with the (100) face exposed to the electrolyte. A single charge, $q_R = -e$ is located at $(0, 0, z)$ in the space between the two electrodes.

Figure 3 shows the force experienced by the test charge in System I as it is moved from one electrode to the other for $V_0 = 0.0V$ (solid line) and $V_0 = 2.75V$ dashed line. The circle and squares are for the same system and conditions respectively, for the method of Reed et al[12]. The proposed method reproduces the force for the cell at the non-zero potential. The force for the zero applied potential case deviates slightly near the electrode surface. The current method uses point charges to represent the electrode surface charge, where the method of Reed et al. uses Gaussian charge distributions centered about the electrode atom

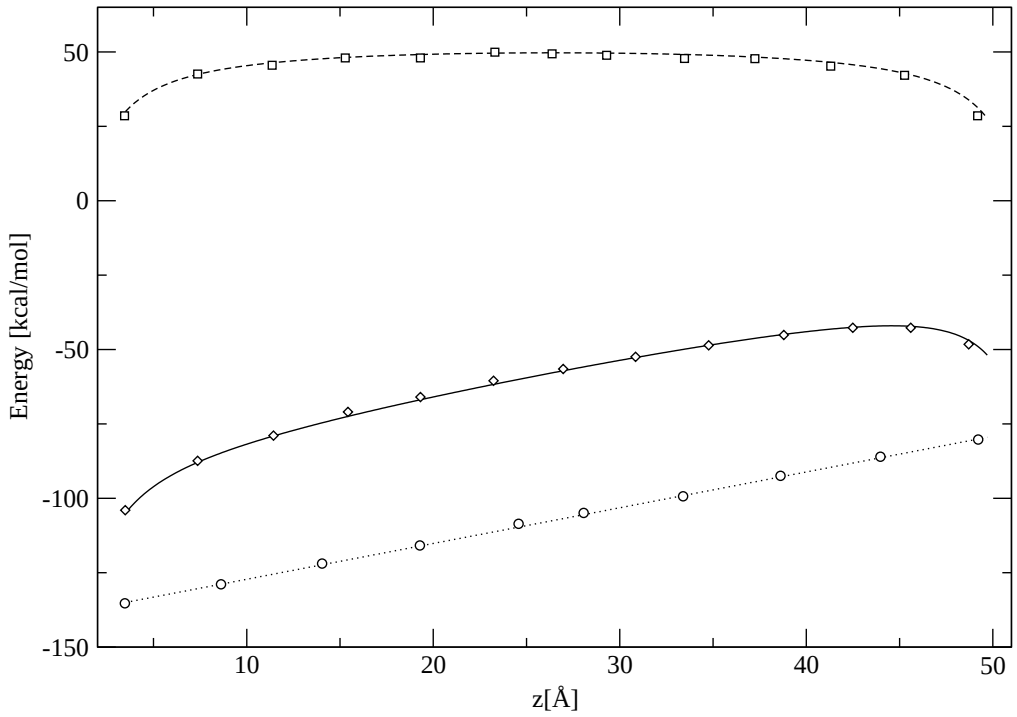

FIG. 4: Energy of System I as a function of the test charge position within the cell. Propose method (lines), and the method, of Reed et al. (symbols). Total energy (solid line and diamonds), the energy due to V_0 (dotted line and circles), and the energy from all images (dashed line and squares).

centers. This may explain the difference at close separation. However, the force for the non-zero applied potential should have the same shape as that for the zero applied potential case, albeit shifted downward to more negative values of force. This is the case for the proposed method, but it doesn't appear to be so for the method of Reed et al. It is unclear why this is.

Figure 4 gives components of the total energy for System I as the test charge is moved across the cell. The dotted line shows that portion of the energy due to the constant potential drop across the cell (Equation 11). Note the distance dependence, that is the constant slope across the cell. This is the reason the shape of the $V_0 = 0.0V$ and $V_0 = 2.75V$ force curves in Figure 3 are identical, albeit shifted by a constant force - that force simply being the slope of the V_0 line in Figure 4. The dashed line of Figure 4 is the component of the energy due to the interaction of the test charge and all images, including the higher order images induced by the primary images of the opposing electrodes. The solid line is the total energy

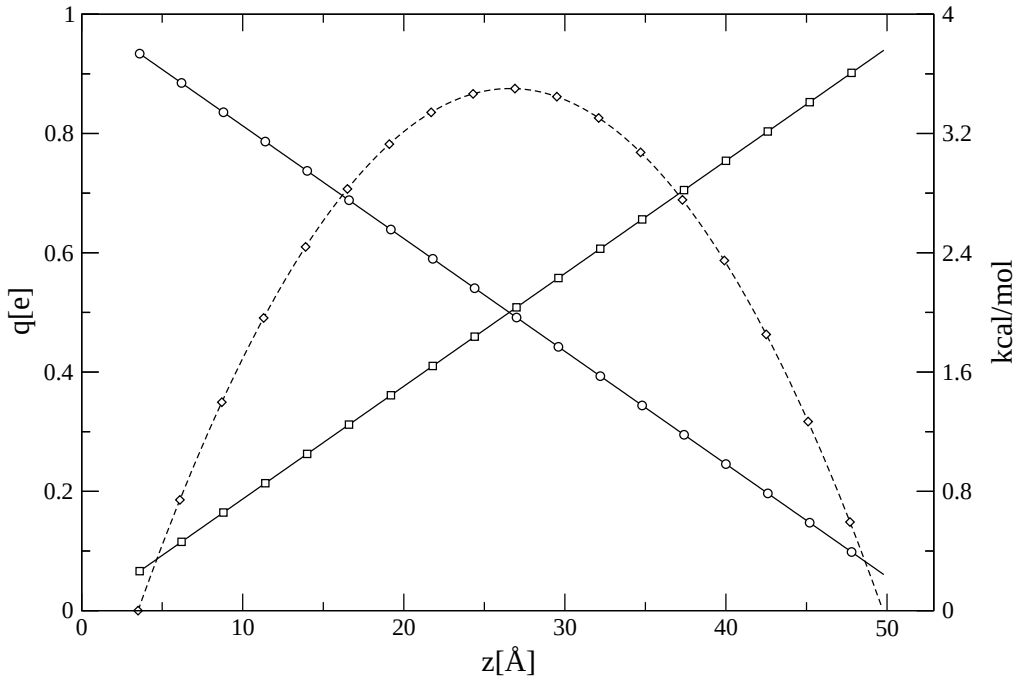

FIG. 5: Electrode charges and interaction energy of System I due to the higher order image charges as a function of test charge position. The surface charge on LE (squares), located at $z = 0$, and charge on RE, located at $z = D$ (circles), and the energy due to the interaction of the test charge with this electrode surface charge (diamonds).

of the system. The symbols are for the method of Reed et al[12]. It can be seen that the proposed method is in excellent quantitative agreement. Most noteworthy is the agreement for the energy due to all images, primary and higher. This is significant because this includes the energy from the higher order image charges that are calculated from Equations 13, and further assumed to be uniformly distributed across the electrode surface (as discussed in relation to Figure 2).

As discussed above, the net surface charge induced on an electrode from these higher order image charges is a function of the position of the electrolyte charges in the cell. Figure 5 shows the way the surface charge due to the higher order image charges varies as the test charge is moved across the cell. By way of an example of the consequences of the variable charge scheme , consider this cell when the test charge is located at $z = \frac{1}{4}D$. From Equations 13 we see that $q_{EL} = \frac{1}{4}q_R$ and $q_{ER} = \frac{3}{4}q_R$. The total charge on LE, *including* the primary image charge ($q_I = -q_R$), is then $-\frac{3}{4}q_R$, and the total charge on RE is $-\frac{1}{4}q_R$. Note that the total charge of the cell remains neutral for any value of q_R.

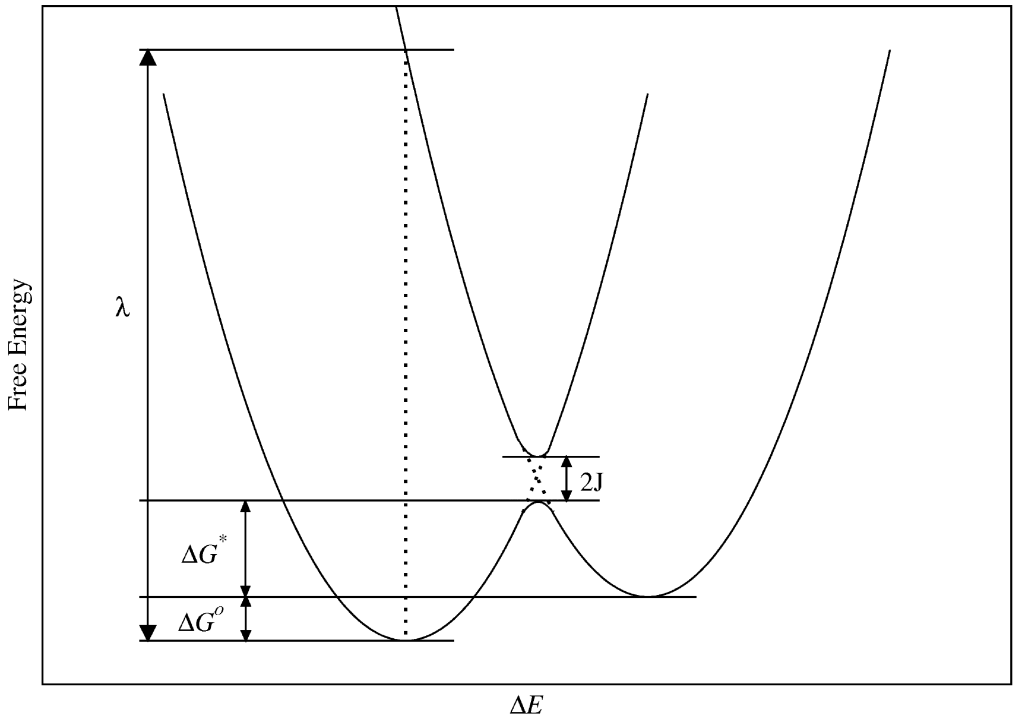

FIG. 6: Representation of Marcus diabatic energy surfaces for two oxidation states.

With the details of the proposed method in place, we next focus on extracting electron transfer rate information from the model using the framework of Marcus theory[16, 17]

C. Electron Transfer

The motivation for the following section is to identify the key values from the preceding method which will allow the calculation of electrode-reactant distance dependent reaction rates for use in a kinetic Monte Carlo (KMC) simulation scheme. Consider two energy surfaces representing the collective coordinates of solvent surrounding an ion with two possible oxidation states, Figure 6. The rate of electron transfer,

$$k_{et} = Ae^{(-\Delta G^*/k_B T)}, \tag{14}$$

can be expressed[16, 17] in terms of the reorganization energy, λ, the free energy of reaction, $-\Delta G^0$, and the pre-exponential factor, A, such that,

$$\Delta G^* = \frac{(\lambda + \Delta G^0)^2}{4\lambda}, \tag{15}$$

and,

$$A = \frac{2\pi}{\hbar}|J|^2 \frac{1}{\sqrt{4\pi\lambda k_B T}}. \tag{16}$$

Assuming linear response of the solvent for the electron transfer reaction - that is, the curves of Figure 6 are quadratic - the mean values of the reaction coordinate for the oxidation and reduction reactions ,$\langle \Delta E_1 \rangle$ and $\langle \Delta E_2 \rangle$ respectively, are related to the difference in the minimas of the free energy for the reaction such that,

$$\Delta G^0 = \frac{1}{2}(\langle \Delta E_1 \rangle + \langle \Delta E_2 \rangle), \tag{17}$$

and the reorganization energy,

$$\lambda = \frac{1}{2}(\langle \Delta E_1 \rangle - \langle \Delta E_2 \rangle). \tag{18}$$

The energy difference between the initial and final states of the reaction can be found using the proposed method of the preceding section. The energy difference for the oxidation reaction, $\delta E_{Red \rightarrow Ox + e^-}$, can be found by selecting some *Red* atom in a molecular dynamics trajectory and calculating the system energy according to the proposed method. The *Red* atom is then changed to the Ox species (with all nuclear coordinates remaining fixed), and the system energy is again calculated according to the proposed method. The energy gap coordinate, ΔE, is simply this energy difference combined with the ionization energy for the ion and the work function of the metal electrode,

$$\Delta E_1 = \delta E_{Red \rightarrow Ox + e^-} + I + W. \tag{19}$$

Since the ionization energy and work functions are constants, $\langle \Delta E_1 \rangle$ can be found by averaging $\delta E_{Red \rightarrow Ox + e^-}$ over many nuclear configurations of a molecular dynamics trajectory. Reed et al. have shown[13] that, on average, the energy difference for the redox species is independent of the electrolyte and is simply the energy for creating the same charge in an otherwise empty cell. This is easily rationalized considering that during the electron transfer process the nuclear coordinates are not allowed to relax, and therefore screen the newly created image charge. It is the image charge that is solely responsible for the average energy difference.

Figure 7 shows the average energy of the oxidation/reduction of a single ion, $M^+ \rightleftharpoons M^{2+} + e^-$, at $V_0 = 10.9V$ for System II described in the validation section. The lines are

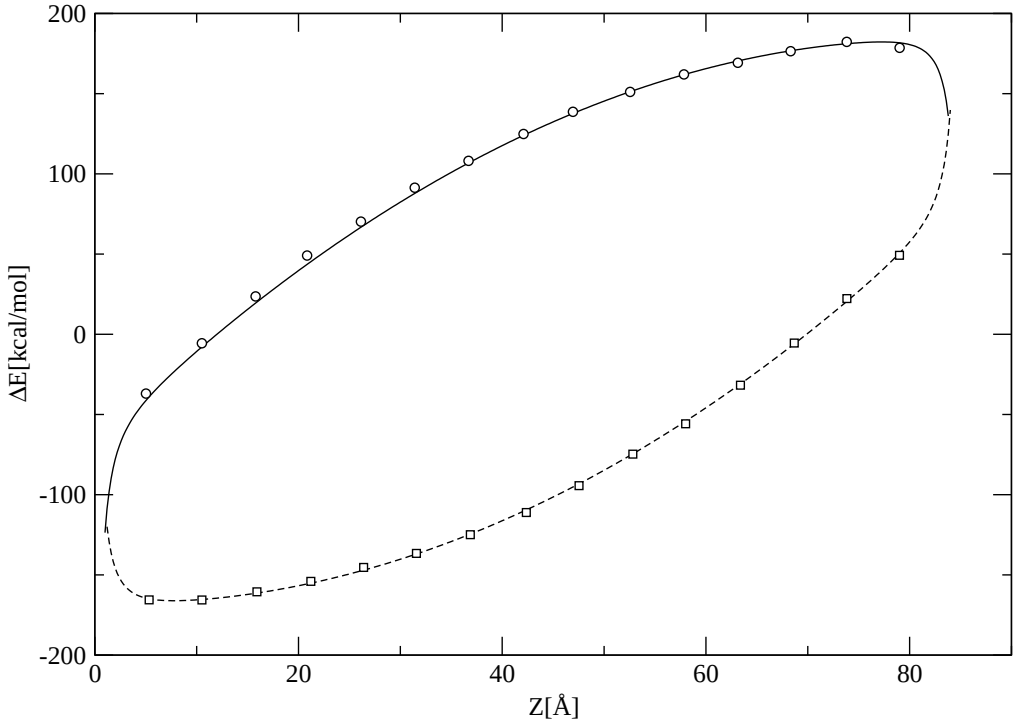

FIG. 7: ΔE for the reduction reaction (solid line, circles), and oxidation (dashed line, squares). The data for the symbols are from Reed et al[13].

data calculated from the proposed method while the symbols are those of Reed et al[13]. Again, the two methods are in excellent agreement.

---

[1] S. Lamperski and J. Klos, The Journal of Chemical Physics **129**, 164503 (pages 7) (2008), URL `http://link.aip.org/link/?JCP/129/164503/1`.

[2] J. B. Straus, A. Calhoun, and G. A. Voth, The Journal of Chemical Physics **102**, 529 (1995), URL `http://link.aip.org/link/?JCP/102/529/1`.

[3] A. Calhoun and G. A. Voth, The Journal of Physical Chemistry **100**, 10746 (1996), http://pubs.acs.org/doi/pdf/10.1021/jp960603q, URL `http://pubs.acs.org/doi/abs/10.1021/jp960603q`.

[4] P. S. Crozier, R. L. Rowley, and D. Henderson, The Journal of Chemical Physics **113**, 9202 (2000), URL `http://link.aip.org/link/?JCP/113/9202/1`.

[5] M. V. Fedorov and A. A. Kornyshev, The Journal of Physical Chemistry B **112**, 11868 (2008), http://pubs.acs.org/doi/pdf/10.1021/jp803440q, URL `http://pubs.acs.org/doi/abs/10.`

1021/jp803440q.

[6] G. Feng, J. S. Zhang, and R. Qiao, The Journal of Physical Chemistry C **113**, 4549 (2009), http://pubs.acs.org/doi/pdf/10.1021/jp809900w, URL http://pubs.acs.org/doi/abs/10.1021/jp809900w.

[7] E. Wernersson and R. Kjellander, The Journal of Chemical Physics **125**, 154702 (pages 9) (2006), URL http://link.aip.org/link/?JCP/125/154702/1.

[8] M. R. Philpott and J. N. Glosli, Journal of The Electrochemical Society **142**, L25 (1995), URL http://link.aip.org/link/?JES/142/L25/1.

[9] E. S. mail: eckhard.spohr@chemie.uni ulm.de, Electrochimica Acta **44**, 1697 (1999), ISSN 0013-4686, URL http://www.sciencedirect.com/science/article/B6TG0-3VDXPHT-2/2/e662fd20e99270f9469518e43cfde1b9.

[10] J. N. Glosli and M. R. Philpott, Electrochimica Acta **41**, 2145 (1996), ISSN 0013-4686, double Layer Modeling, URL http://www.sciencedirect.com/science/article/B6TG0-3V9CRVF-9/2/157c16779393b95655ee8d43616f9b59.

[11] J. I. Siepmann and M. Sprik, The Journal of Chemical Physics **102**, 511 (1995), URL http://link.aip.org/link/?JCP/102/511/1.

[12] S. K. Reed, O. J. Lanning, and P. A. Madden, The Journal of Chemical Physics **126**, 084704 (pages 13) (2007), URL http://link.aip.org/link/?JCP/126/084704/1.

[13] S. K. Reed, P. A. Madden, and A. Papadopoulos, The Journal of Chemical Physics **128**, 124701 (pages 10) (2008), URL http://link.aip.org/link/?JCP/128/124701/1.

[14] D. J. Griffiths, *Introduction to Electrodynamics (3rd Edition)* (Benjamin Cummings, 1998), ISBN 9780138053260.

[15] E. Spohr, The Journal of Chemical Physics **107**, 6342 (1997), URL http://link.aip.org/link/?JCP/107/6342/1.

[16] R. A. Marcus, The Journal of Chemical Physics **24**, 966 (1956), URL http://link.aip.org/link/?JCP/24/966/1.

[17] R. A. Marcus and N. Sutin, Biochimica et Biophysica Acta (BBA) - Reviews on Bioenergetics **811**, 265 (1985), ISSN 0304-4173, URL http://www.sciencedirect.com/science/article/B758C-47VJ7X5-2V/2/212a2010fabb6c49988711633106ae29.